Using Deep Learning for Radiation Therapy and Response Prediction

B. Ibragimov, D. Toesca, W. Zhao, Y. Wu, A. Koong, D. Chang, L. Xing

Departments of Radiation Oncology, Stanford University

Stanford University
Department of Radiation Oncology
School of Medicine

Disclosures

- Dr. Lei Xing has received speakers honoraria from Varian Medical Systems.
- Research grants supports from NIH, Varian, Google Inc., Huyihuiying Medical Co, Siemens.
- Scientific adversor for Huiyihuiying Medical Co.
- Founder of Luca Medical Systems.

Learning from data

- Supervised learning
- Unsupervised learning
- Reinforcement learning

Stanford University
Department of Radiation Oncology
School of Medicine

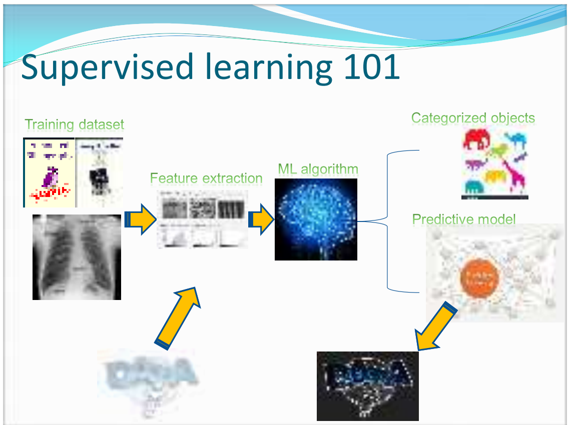
Supervised learning 101
Training dataset
Feature extraction
ML algorithm
Categorized objects
Predictive model

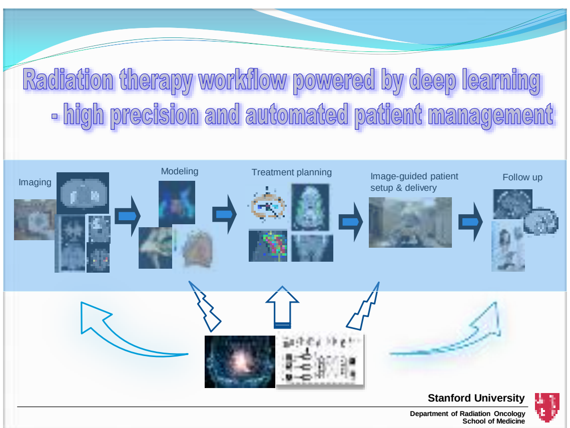
Radiation therapy workflow powered by deep learning
- high precision and automated patient management
Imaging
Modeling
Treatment planning
Image-guided patient setup & delivery
Follow up
Stanford University
Department of Radiation Oncology
School of Medicine

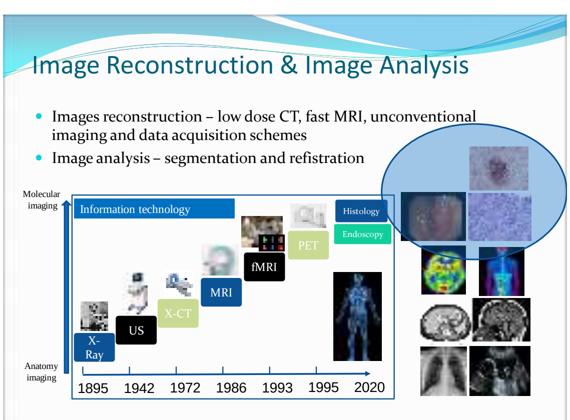
Image Reconstruction & Image Analysis
Images reconstruction – low dose CT, fast MRI, unconventional imaging and data acquisition schemes
Image analysis – segmentation and refistration
Molecular imaging
Anatomy imaging
Information technology
Histology
Endoscopy
PET
fMRI
MRI
X-CT
US
X-Ray
1895
1942
1972
1986
1993
1995
2020

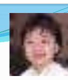

Sparse Data Image Reconstruction using U-net

Y Wu et al, TMI, submitted, 2018

- Data Sampling
  - Raw data are sampled point by point in Fourier domain (k-space)
- Image Reconstruction
  - Inverse Fourier transform is applied on the raw data to generate output in the image domain

Inverse Fourier Transform

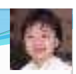

Volumetric deep learning for super-resolution MRI

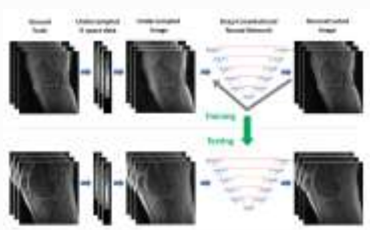

Also see - Mardani M, Gong E, Cheng J.YY, Vasanawala S.S, Xing L, and Pauly J. M, Deep generative adversarial networks (GAN) for MRI, *IEEE Trans Med Ima 37, in press*, 2018.

Stanford University
Department of Radiation Oncology
School of Medicine

Generative Adversarial Networks (GANs) for Compressive Sensing and Real-Time MRI

- *k*-space data model

$$\mathbf{y} = \underbrace{\Phi}_{M \times N}\mathbf{x}$$

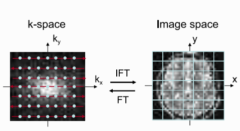

- Problem: Given the training data $\{(\mathbf{x}_i, \mathbf{y}_i)\}_{i=1}^{N}$, and the current *k*-space data $\mathbf{y}$,
  - retrieve the image $\mathbf{x}$
  - in real-time when *M* << *N*

M. Mardani, L. Xing, J Pauly,

Stanford University
Department of Radiation Oncology
School of Medicine

Integrated MRI-Radiation therapy Systems:
MRI Guided Localization & Delivery

Courtesy of Jihong Wang

Types of learning

- Supervised learning
- Unsupervised learning
- Reinforcement learning

Stanford University
Department of Radiation Oncology
School of Medicine

Radiation therapy trajectory optimization
(S. Kahn, B. Fahimian ….)

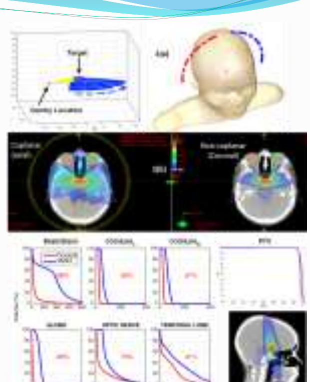

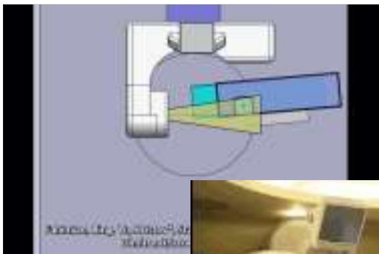

Trajectory Optimization for VMAT

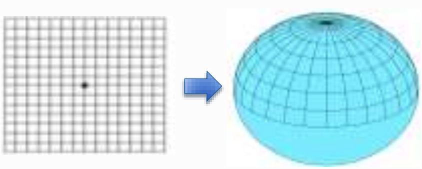

Decision: A trajectory of stone positions

Decision: A trajectory of Gantry angle, and Couch angle

Dong P & Xing L, Physics in Medicine & Biology, in press, 2018

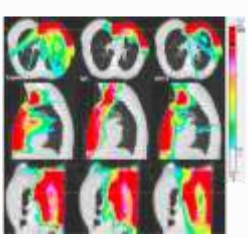

Compared with coplanar:

- *Heart mean dose:* reduced from 15 Gy to 7 Gy *Heart V30:* reduced from 7.5% to 1.7%.
- *Left and right lung mean doses:* reduced from 16 Gy and 8 Gy to 11 Gy and 3 Gy, respectively

Compared with 4pi:

- MCTS spares spares more on ipsilateral lung, heart and contralateral breast.
- Contralateral lung is better spared in the 4pi plan.

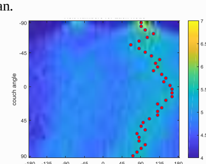

Dong P & Xing L, Physics in Medicine & Biology, in press, 2018

DLGRT delivery

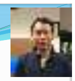

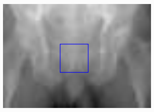

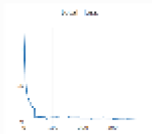

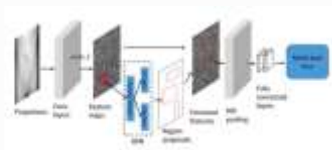

Zhao W, et al, 2018 AAPM Annual Meeting, Thursday

Beam level imaging

Visualizing the invisible soft tissue target

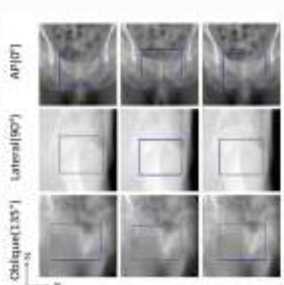

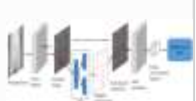

Zhao W, et al, RADIOLOGY, Submitted, 2018

From population-average nomogram to deep learning-based toxicity prediction

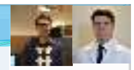

— B. Ibrimbrov, D. Toesca, D. Chang, A Koong, L Xing

Current approach:

(i) radiomics;

(ii) NTCP/TCP types of modeling

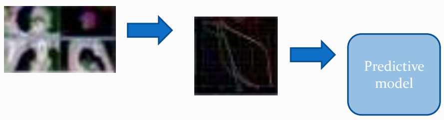

Problems: biological heterogeneity, spatial information

Multi-channel deep dose analysis

20

Multichannel CNNs:

- First channel – 3D anatomy segmentation
- Second channel – 3D dose plan
- Third channel – CT image

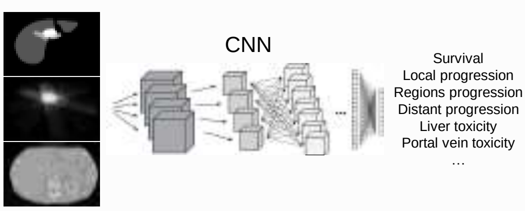

ROC curves for the deep learning-based and existing DVH-based toxicity predictors

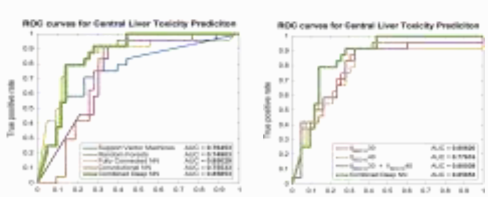

(a) All SVM, RFs, FcNNs, CNNs and hybrid DNN predictors achieved AUC > 0.7. (b) The hybrid DNN predictor with AUC of 0.859 outperforms the existing DVH-based predictors $V_{BED10}30$, $V_{BED10}40$ and $V_{BED10}30$ U $V_{BED10}40$. B Ibragimov et al, submitted, 2018

Deep dose analysis: numerical features

22

Demographics
Gender
Age

Liver comorbidities
Chronic cirrhosis
Chronic HBV
Chronic HCV

Lab measurements
Albumin
Bilirubin
Aspartate transaminase
Alanine transaminase
Alkaline phosphatase
Alpha-fetoprotein
Sodium
Creatine
Platelets

Liver therapies
Tumor resection
Chemoembolization
Prior chemotherapy
Post-RT chemotherapy
Biliary stent
SRBT dose
SBRT fractions

Anatomy
tumors
Max tumor radius
GTV
PTV
Liver volume
Hepatobiliary tract volume

Deep dose analysis: combined

23

Multi-path network: 1) 3D CNN for dose plan; 2) fully-connected path for features

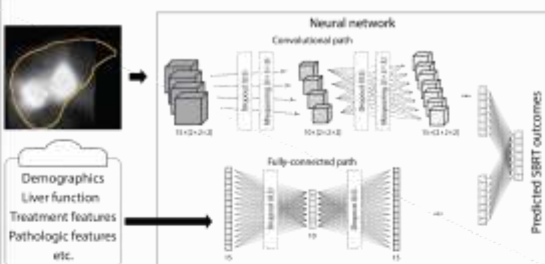

Deep dose analysis: survival results

Results:

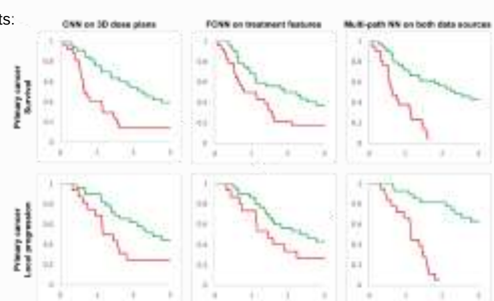

Green – patients with positive predicted outcome, Red – patients with negative predicted outcome

Deep dose analysis: survival results

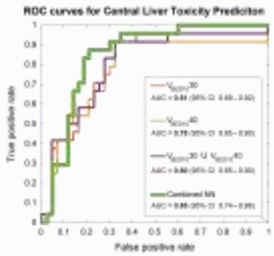

Magical deep learning box

Problem: 3D dose plan + Image analysis → → Prediction

Radiation-sensitivity atlas

Survival and local progression atlas:

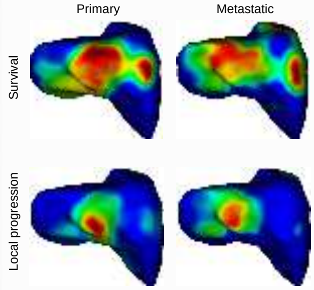

Results:

- Atlases agree for primary cancer (*correlation coef. = 0.56*)
- Atlases agree for metastatic cancer (*correlation coef. = 0.85*)
- Disagree between each other (*correlation coef. = 0.19*)
- Highest risks are for liver segment I, where liver vasculature is located
- Lowest risks are for liver segments II, V and VIII

Radiation-sensitivity atlas

Hepatobiliary toxicity atlas:

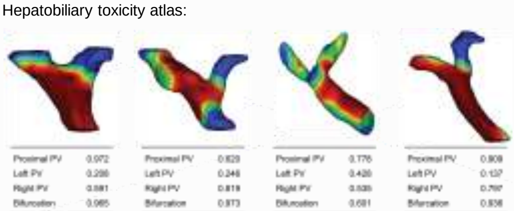

Results:

- Risks for left vein are 2-times lower than risks for right vein
- Left vein supports 1/3 of the liver, while right vein supports 2/3 of the liver

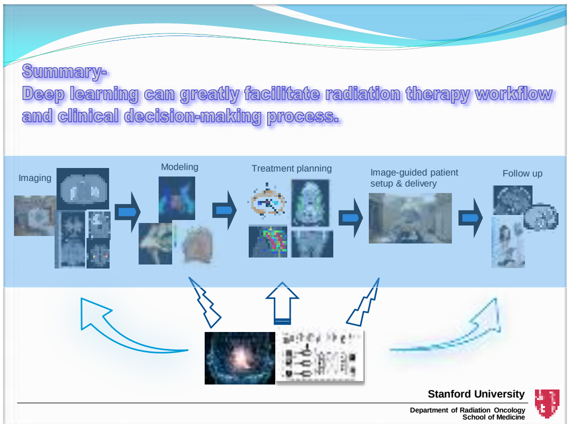

Acknowledgement

- B. Ibragimov, Y. Wu, Y. Yuan, W. Zhao, W. Qin, H. Liu, M. Korani, D. Li, K. Cheng, C. Jenkins, S. Tzoumas, D. Vernekohl, I. Patel, P. Dong, B. Ungan
- A. Koong, D. Chang, D. Toesca, B. Han, Y. Yang, Q. Le, S. Soltys, J. Pauly, S. Boyd
- Funding: NIH/NCI/NIBIB, DOD, NSF, ACS, RSNA, Varian, Siemens, Google, HuiYiHuiYing, NVIDIA.